European Cooperation in the field of Scientific and Technical Research

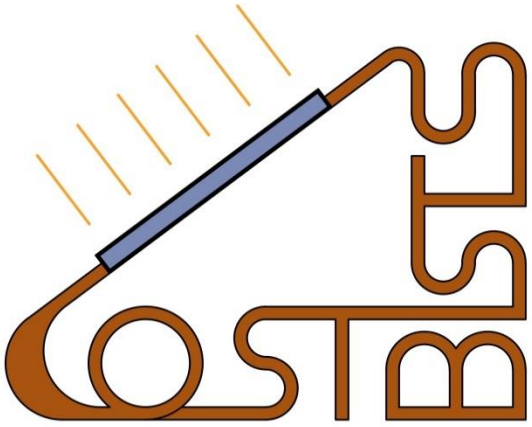

COST Action TU1205 (BISTS)

Building Integration of Solar Thermal Systems

Title:

D 2.6 Report on the development of new models for innovative integrated STS applications

COST is supported by

ESF provides the COST Office and

Date: April, 2017

Contributors: A. Moreno, A. Riverola, D. Chemisana, I. Visa, A. Duta, M. Moldovan and M. Comsit

Contents:

Abstract

A building integrated solar thermal (BIST) collector has been modelled and simulated. The BIST system has been placed in the south façade, covering 50% of the façade area. The BIST collector has been evaluated in terms of the contribution to domestic hot water and to space heating. In addition, the impact on the building thermal demand has been analysed.

The dynamic simulation has been carried out in TRNSYS 16. This allows understanding and analyzing the synergies between the solar collector and the building, and how these two interact. Approach A of Maurer et al. has been used for modelling the energetic behaviour of the BIST module and the building envelope in seven different countries.

The annual reduction of thermal demand compared to the building without a BIST system is around 6.60% in Spain, 9.92% in Italy, 5.38% in Romania, 5.04% in Austria, 10.30% in France, 5.68% in Germany and 2.62% in Finland. In the case of domestic hot water energy demand, which has been considered a priority, the calculated average solar fractions are around 94.30% in Spain, 93.80% in Italy, 90.45% in Romania, 85.52% in Austria, 84.00% in France, 81.00% in Germany and 74.00% in Finland. On the other hand, the proposed system covers part of the space heating demand, resulting in a solar fraction in the period from October to March of 11.90% in Spain, 9.00% in Italy, 6.00% in Romania 4.21% in Austria, 4.20% in France, 3.90% in Germany and 2.6% in Finland.

1. Introduction

Buildings account for 40 % of the total energy consumption in the European Union [1]. Therefore, in the years to come, it is key to reduce this consumption and to supply energy from renewable sources. This combined with a series of optimised and well balanced operations between consumption and production coupled with successful grid integration are the basis of nearly zero-energy buildings (NZEBs) [2]. The trend toward low-energy buildings is also supported by more stringent legal requirements on existing and new buildings and the increasing value of such buildings as real estate. In this context, the European Directive on The Energy Performance of Buildings requires all new buildings to be (NZEBs) by the end of 2020 and all new public buildings by 2018 [1], allowing to reduce the Union's energy dependency and greenhouse gas emissions. Solar energy is a promising and powerful source of energy that can be used to heat, cool and light our homes and businesses. It is well known that the sun delivers more energy to the earth in one hour than the world's energy consumption in one year [3]. Within solar systems, active solar building envelopes could potentially play an important role in the future energy system based on renewable energy sources. Building-integrated solar systems (BISS) are cheaper than the building envelope and solar system separately, since the price of materials and labour together is lower. Building-integrated photovoltaic (BIPV) and solar-thermal (BIST) systems are two examples of available systems for constructing active solar building envelopes [4].

A BIST system is depicted in Fig 1.1. When a solar collector is integrated as a part of a building envelope, the thermal performance of both the collector and the building component are changed. The building envelope influences the collector back heat losses and consequently alters its efficiency; on the other

hand, the heat fluxes of the building envelope must be re-evaluated considering the solar collector as part of the envelope itself [5]. There are a lot of works about the influence on the solar systems performance when integrated in buildings, whereas there are just a few studies that analyse the influence in the building envelope.

Maurer et al. [6] present different modelling approaches which can be used as approximations for certain situations. Different methodologies were used to derive these approaches. Approach A is recommended for BIST collectors with good insulation towards the building interior. The efficiency curve is modified to account for reduced back losses. Approach B is recommended if the heat flux from the absorber to the building is important. A conventional collector model is used and the outputs are modified to account for the thermal coupling between the collector and the building. Approach C can be used, for example, when the solar thermal performance is monitored and available. The extended efficiency curve increases the calculation accuracy for the solar thermal performance. Approach D is recommended if measurements of the energy flux to the building interior and of the solar thermal performance e.g. on a test facility are available. The necessary data and effort increase from Approach A to Approach D, as does the accuracy of the models.

The goal of this study is to understand and analyse the synergy between the solar collector and the building, and how these two interact. A dynamic simulation of a solar thermal collector designed for integration on the façade of buildings is presented. Approach A of Maurer et al. has been used for modelling the energetic behaviour of the BIST system and the building envelope in seven countries. In order to determine the level of insulation of buildings walls for each country, the reference values reported in the corresponding normative were retrieved.

Energetic dynamic simulations have been carried out in TRNSYS 16 and the building model was created with TRNBuild. The analysed system consists of three principal subsystems: (i) building, occupancy and weather data, (ii) solar-thermal subsystem and (iii) solar domestic hot water (DHW) and space-heating subsystem.

The deliverable is divided in 4 sections. In the next section, a description of the BIST system is presented. This is followed by section 3 that introduces the methodology employed. Finally, the results and conclusions are presented in sections 4 and 5 respectively.

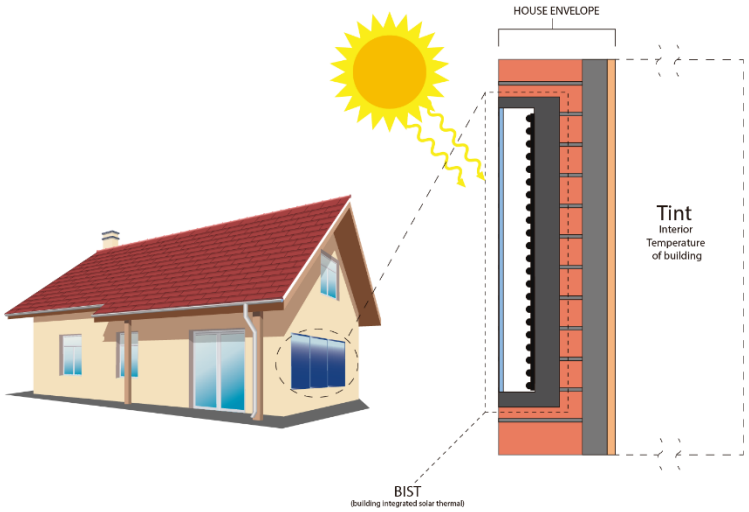

Figure 1.1 Picture representation of the BIST (building integrated solar thermal)

2. BIST collector description

The collector is designed mainly for developing arrays implemented in facades with increased architectural acceptance. Therefore, colours like red, green, blue are targeted for the absorber plate, along with the conventional black, as shown in the schematic description of the collector reported in Fig.2.1. The isosceles trapeze shape collector is used to heat or pre-heat water for building heating and domestic hot water purposes.

Figure 2.1 Novel trapeze solar-thermal flat plate collector

The collector has an active area of 0.67m^2 and it consists of a cover, an absorber, meander tubes, and insulation at the backend and edges of the collector. The cover glass has high optical absorptance and it is used for reducing both radiation and convection losses from the collector. The absorber plate is made of an aluminium substrate with a spectral selective black non-reflective coating. The fluid, heated by the absorber, is circulated in the meander tubes, bonded to the absorber plate by copper clamps. Conduction

losses from the backend and edges of the collector are reduced by insulation: a layer of mineral wool is placed on the back plate, while a layer of polyurethane is placed around the frame. The main prototype design features are summarized in table 2.1. More information of the solar collector can be found in reference [7].

Glass cover optical absorptance [-]	0.89	**Absorber plate conductivity [W/m K]**	205
Glass cover emittance [-]	0.88	**Absorber plate emissivity [-]**	0.11
Glass cover thickness [mm]	4	**Absorber plate absorptance [-]**	0.887
Wool insulation thickness [mm]	45	**Air gap thickness [mm]**	20
Wool insulation conductivity [W/mK]	0.045	**Tubes diameter [mm]**	22.7/10.7
Polyurethane insulation thickness [mm]	20	**Number of tubes [-]**	9

Table 2.1 Principal characteristics of Novel trapeze solar-thermal flat plate collector

This novel trapeze flat plate solar thermal collector was designed and developed as a building block for "lego-type" solar-thermal facades, with various geometries. Groups of three trapeze collectors serially interconnected in various configurations were proposed [8] to cope with specific architectural prerequisites of the facades. The main goal was to improve the architectural acceptance of the solar facade while increasing the coverage degree of the facade with solar thermal collectors. Thus, the surface covered with trapeze solar collectors can be three times larger than in the case of rectangular ones.

To evaluate the influence of serially and/or parallely hydraulic interconnections between the novel trapeze flat plate solar thermal collectors, a solar thermal façade was developed and implemented (Fig. 2.2) in a temperate-continental mountain climate (Brasov, Romania: 45°40'08.6"N, 25°32'57.8"E, 600 m above the sea level). Novel trapeze and commercial rectangular solar thermal collector are installed both in vertical position on the southern façade and optimally tilted on the rooftop. Novel trapeze collectors 1, 2 and 3 are parallely connected, and the other six collectors (4 to 9) are serially connected as presented in Fig. 2.2. A commercial flat plate solar collector (10) is also installed on the façade allowing comparison studies on the output thermal energy and efficiencies.

Figure. 2.2 Outdoor testing rig with flexible interconnection of the novel trapeze solar-thermal flat plate collectors

Vertical position of the solar thermal collectors increases the amount of the thermal energy output during the winter time in comparison with the optimal tilted ones, which is beneficial for the solar fraction; during the summer time, the thermal energy output is lowered due to the lower received solar energy in the vertical plane, thus, the overheating of the large surface of the solar façade is prevented. Groups of three serially interconnected collectors are efficient, infield thermal energy response is close to the nominal efficiency, particularly during the cold and mild months. Seasonal changes in the collectors' interconnection are also experimentally evaluated to optimise the outlet temperature.

3. Methodology

The energetic simulation has been conducted in TRNSYS 16. The performance of the BIST system under energy demands due to space-heating and DHW has been evaluated. Also to compute the influence on the building envelope, a thermal simulation has been carried with TRNBUILD. All the simulations are linked together into the same model. In Fig. 3.1, the main elements which have been taken into account are depicted. These are the solar collectors with type1b, the tank with type 534, and the house thermal demand with type 56.

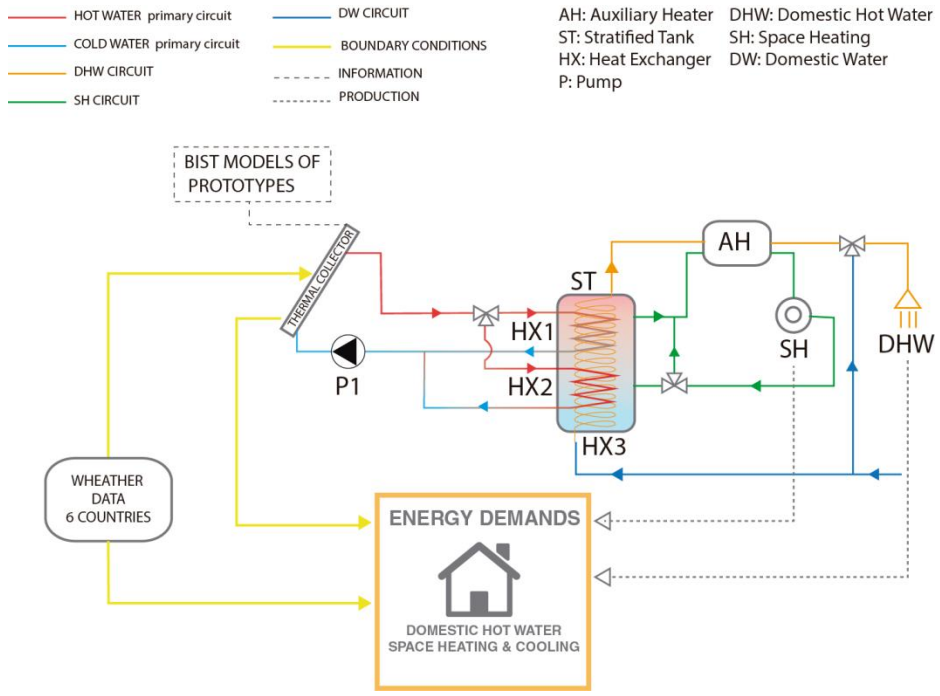

Figure 3.1 Simulated system typology

In the next sub-sections, first a sensitivity analysis of the weather has been carried out, after the performance of the BIST has been estimated and finally the thermal model of the building has been defined.

3.1. Reference climate data

Energy simulation programs have a wide variety of weather data from which to choose, from locally recorded weather data to preselected 'typical' years. Different definitions and hence different types of data sets are available (IWEC, TRY, TMY, Meteonorm, etc.) based on different weighting of the parameters and other choices. Weather data sets can be in the form of hourly data (8760 hours per year) synthesized to represent long-term statistical trends and patterns. They are used for hourly calculations of energy and power demand of buildings.

First, a comparison of the available climatological data (IWEC, METEONORM) has been performed. The mean temperatures and global irradiance have been analysed on a horizontal surface in several cities in order to evaluate the differences between different weather sources. The results are reported in Table 3.1. All the selected cities are the capital of their respective countries.

Country	SOURCE	End-use	Jan	Feb	Mar	Apr	May	Jun	Jul	Aug	Sep	Oct	Nov	Dec	Annual
ES Madrid	IWEC	Tmean [ºC]	6.2	7.4	9.9	12.2	16.0	20.7	24.4	23.9	20.5	14.8	9.4	6.4	13.5
		G [kW/m²]	58.2	74.5	117.2	145.1	184.0	199.1	222.7	198.4	143.1	101.3	63.9	51.4	1559.0
	METEO.	Tmean [ºC]	5.4	7.0	9.3	11.4	15.6	20.1	24.3	23.9	20.0	14.5	8.8	6.0	13.0
		G [kW/m²]	66.0	77.3	141.3	152.4	203.7	223.0	229.6	200.6	150.2	104.5	64.0	49.0	1661.7
IT Rome	IWEC	Tmean [ºC]	8.3	9.0	10.6	13.3	17.6	21.2	24.2	24.4	21.5	17.0	12.8	9.4	15.1
		G [kW/m²]	50.4	71.8	114.8	140.1	178.6	190.1	210.9	179.6	133.3	89.1	57.2	45.8	1461.7
	METEO.	Tmean [ºC]	8.0	8.8	10.8	13.2	17.4	21.0	24.1	23.9	20.6	16.9	12.1	9.3	15.0
		G [kW/m²]	57.5	72.8	122.4	154.0	191.8	202.4	215.7	189.1	142.0	100.8	63.0	49.3	1560.9
RO Bucharest	IWEC	Tmean [ºC]	-1.7	0.8	5.0	11.4	16.5	20.4	22.7	21.8	16.2	11.2	4.5	0.1	11.3
		G [kW/m²]	39.4	65.7	103.5	136.0	181.2	192.9	204.0	179.6	124.9	83.3	44.0	34.6	1389.1
	METEO.	Tmean [ºC]	-	-	-	-	-	-	-	-	-	-	-	-	-
		G [kW/m²]	-	-	-	-	-	-	-	-	-	-	-	-	-
AT Vienna	IWEC	Tmean [ºC]	-0.1	-0.5	5.3	10.6	15.2	17.3	20.2	20.0	15.5	10.8	4.7	-0.2	10.7
		G [kW/m²]	25.9	44.7	83.3	120.3	155.7	161.5	172.8	154.8	97.2	59.4	27.8	19.0	1122.4
	METEO.	Tmean [ºC]	-1.1	0.9	5.3	9.9	14.4	17.6	19.8	19.2	15.5	10.3	4.4	0.4	10.1
		G [kW/m²]	26.8	42.7	83.2	114.4	157.7	161.0	168.8	144.9	97.1	65.3	29.9	20.2	1112.0
FR Paris	IWEC	Tmean [ºC]	3.9	4.2	7.0	10.0	14.3	16.8	19.4	19.7	15.7	11.3	6.4	4.5	10.7
		G [kW/m²]	24.1	39.0	70.7	108.9	142.8	159.3	166.0	150.8	93.5	63.0	31.3	18.8	1068.1
	METEO.	Tmean [ºC]	2.8	3.2	5.7	8.7	12.6	15.5	17.6	17.3	14.2	10.6	6.0	3.7	9.7
		G [kW/m²]	24.0	41.9	74.2	112.1	136.9	151.1	159.8	137.7	94.8	59.0	32.4	19.3	1043.2
DE Berlin	IWEC	Tmean [ºC]	1.9	0.3	5.4	8.3	14.0	17.6	19.1	18.5	15.0	10.2	4.4	2.4	9.3
		G [kW/m²]	16.4	33.1	59.8	115.2	150.1	151.2	158.4	134.7	82.3	47.9	23.9	12.6	985.5
	METEO.	Tmean [ºC]	-0.2	0.5	4.1	8.5	14.1	17.3	18.9	18.4	14.6	9.9	4.7	1.5	9.2
		G [kW/m²]	18.6	33.6	70.6	107.1	150.2	157.5	156.1	133.7	88.3	50.5	21.6	13.4	1001.1

Table 3.1 Comparison the mean temperature and the horizontal irradiance with IWEC and METEONORM files.

Relative differences between the two sources of climatic data ranging from 0.53% to 9.80% have been observed .This confirms that the election of the source of climatic data can influence the results and it is important to specify which one is the source. In the present work, the dynamic simulation has been performed using the IWEC data files.

3.2. BIST model

The BIST collector has been modelled using the so-called approach A proposed by Maurer et al [6]. In this approach, the insulation between the BIST collector absorber and the building interior is very thick, and therefore, the heat losses from the absorber to the interior can be neglected. The approach that has been proposed to approximate the efficiency curve without back-surface losses, is based on modifications on the non- linear flat-plate collector model suggested by Cooper [9].

The effective transmittance-absorptance product $(\tau\alpha)_e$ is calculated from the transmittance of the cover glazing τ and the absorptance of the absorber α:

$$(\tau\alpha)_e \cong 1.01 \cdot \tau \cdot \alpha \qquad \text{eq. 1}$$

The collector efficiency factor F' can be calculated using the efficiency for zero temperature difference between the average fluid temperature and the ambient temperature:

$$(\tau\alpha)_e \cong 1.01 \cdot \tau \cdot \alpha$$ eq. 2

$$F'_{BAST} = \frac{\eta_{0,BAST}}{(\tau\alpha)_e}$$ eq. 3

The thermal losses of the already absorbed energy at zero temperature difference between the average fluid temperature and the ambient temperature can be expressed as follows:

$$Fraction\ of\ thermal\ losses \rightarrow (1 - F'_{BAST})$$

$$Fraction\ of\ thermal\ losses\ back\ surface \rightarrow \frac{1}{7}(1 - F'_{BAST})$$

Without back-surface losses, the collector efficiency factor of the BIST case (F'BIST) is equal to:

$$F'_{BIST} = F'_{BAST} + (1 + F'_{BAST}) \cdot \frac{1}{7} F'_{BiST}$$ eq. 4

Therefore it is possible to write:

$$F'_{BIST} = \frac{F'_{BAST}}{1 - f_{bl} + f_{bl} F'_{BAST}}$$ eq. 5

The efficiency at zero temperature difference between the average fluid temperature and the ambient temperature in the BIST case and BASE cases are respectively:

$$\eta_{0,BIST} = (\tau\alpha)_e \cdot F'_{BIST}$$ eq. 6

$$\eta_{0,BAST} = a_{1,BAST} \frac{\Delta T_{stag,BAST}}{G} - a_{2,BAST} \frac{\left(\Delta T_{stag,BAST}\right)^2}{G}$$ eq. 7

The right-hand side of this equation is equal to the thermal losses due to stagnation temperature. In the BIST case, the fraction f_{bl} of these losses equals to the BIST efficiency:

$$\eta_{0,BIST}(\Delta T_{stag,BAST}) = \eta_{0,BIST} - a_{1,BIST}\frac{\Delta T_{stag,BAST}}{G} - a_{2,BAST}\frac{(\Delta T_{stag,BAST})^2}{G} \quad \text{eq. 8}$$
$$= (1 - f_{bl})\eta_{0,BAST}$$

Assuming $a_{2,BIST} = a_{2,BAST}$, $a_{1,BIST}$ can be fitted as reported in Table 3.2.:

	η_0	a1	a2
BAST	62.21	2.4052	0.0391
BIST	64.15	2.05	0.0391

Table 3.2 Parameters of the efficiency curves for the BAST and BIST collector .

The thermal characteristic curve of the collector (BAST and BIST) is plotted as a function of the fluid mean temperature and the ambient one divided by the incident radiation, in (Fig. 3.2).

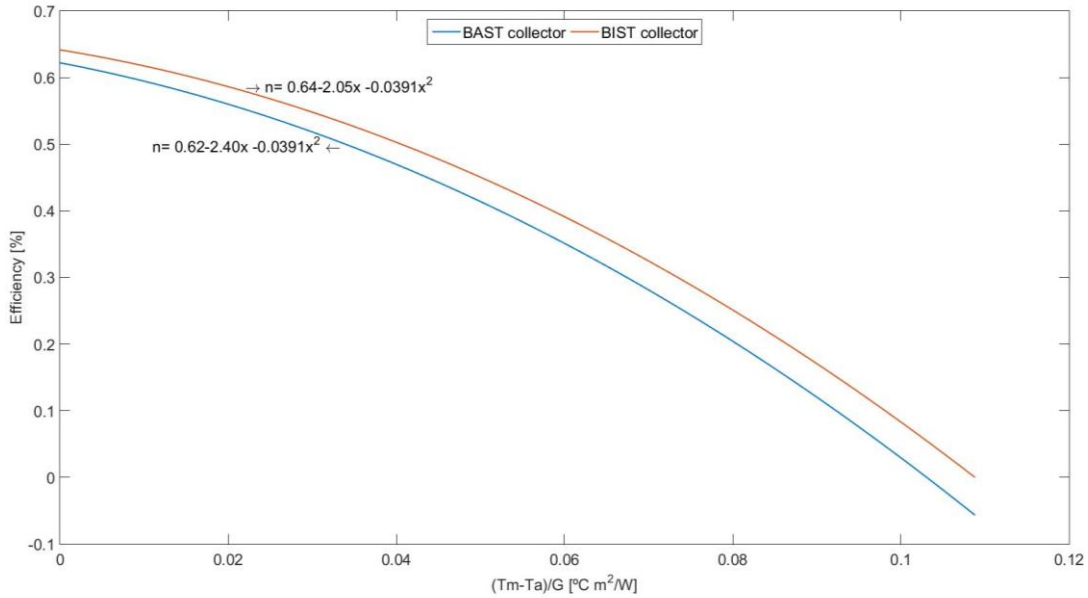

Figure 3.2 Curves of the efficiency for the BAST and BIST collector

3.3. Thermal model of the building

The analysed building with integrated BIST has been selected to be a single family house, composed by two floors over ground level (Fig 3.3). The conditioned surface is 140 m^2 and the ratio surface to volume (S/V) is 0.7. The main geometric characteristics and internal gains are fixed for all the countries and reported in Table 3.2 whereas the thermal characteristics are variable depending on the country. The buildings envelope thermal transmittances for each country are (Table 3.3) based on buildings constructed up to 2008. This values have been extracted from ENTRANZE project, which provides characteristics of buildings in Europe [10]

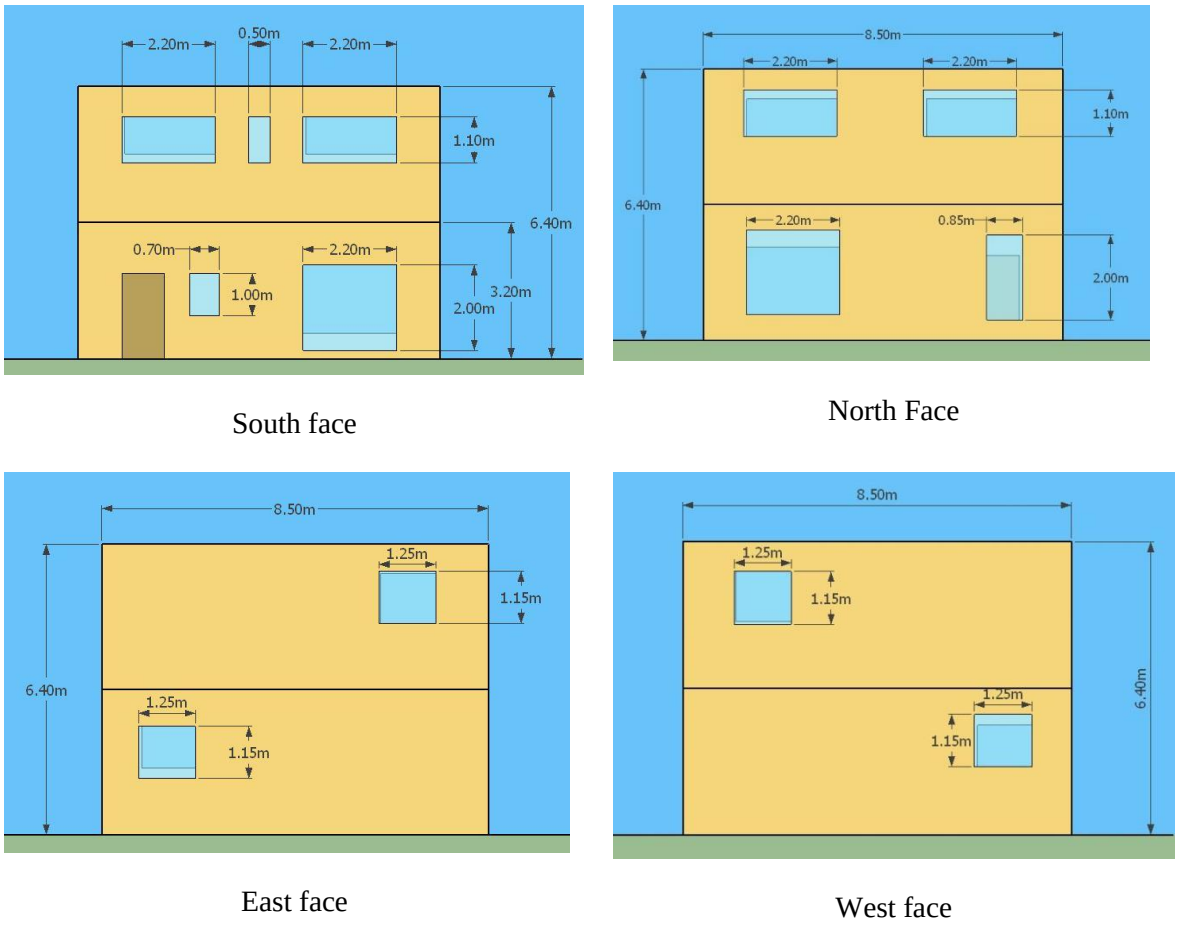

Figure 3.3 Annotations of the building model.

The envelope is composed of three layers: solid brick, insulation and plasterboard (from the exterior to the interior Fig 3.4). The solid brick and plasterboard thicknesses have been kept constant whereas the insulation thickness has been varied to obtain the corresponding thermal transmittance. Regarding the fenestration, the appropriate composition to achieve the desired transmittance and solar factor set has been used.

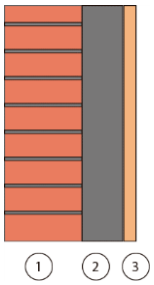

	Material	Density [kg/m^3]	Conductivity [W/m·K]	Heat capacity [J/kg·K]	Thickness [cm]
1	Solid brick	1920	0.72	835	12
2	Wool (insulation)	23	0.038	1800	Parametric
3	Plasterboard	800	0.17	----	1.5

Figure 3.4 Composition of the walls (envelopes)

		All Countries
Building geometry	Nº of heated floor	2
	S/V ratio	0.7 m^2/m^3
	Orientation	S/N
	Net dimensions of heated volume	8.5 x 8.5x 6 m
	Net floor area of heated zones	140 m^2
	Area of S façade	51 m^2
	Area of E façade	51 m^2
	Area of N façade	51 m^2
	Area of W façade	51 m^2
	Area of Roof	72.25 m^2
	Area of Basement	72.25 m^2
	Window area on S façade	25%
	Window area on E façade	7%
	Window area on N façade	25%
	Window area on W façade	7%
Internal gains	People design level	50 m^2/people
	Lighting design level	3.5 W/m^2
	Appliance design level	4 W/m^2

Table 3.2 Fixed characteristics of the building .

	Building construction period (average based on stock)				
	U value of wall	**U value of roof**	**U value of basement**	**U value of window**	**g value of glass**
Spain	1.82	1.19	1.73	4.64	0.7
France	1.73	1.61	1.44	3.55	0.7
Italy	1.52	1.79	1.75	5.20	0.7
Germany	1.11	0.75	0.87	2.87	0.7
Romania	1.58	1.31	1.46	2.42	0.7
Austria	1.06	0.59	1.07	2.20	0.7
Finland	0.43	0.29	0.41	1.96	0.7

Table 3.3 Variable characteristics of the building .

To evaluate the influence of the BIST system in the envelope and to compare in terms of thermal demand, the energy needs for the building variants are calculated assuming the same indoor conditions. An operative temperature of 20°C in winter and of 26°C in summer (latent control not applied) and the same values of minimum air change (at maximum occupation rate), coherent with the assumed occupation levels and the ventilation rates proposed by EN15251, that is 0.5h-1 in the residential buildings.

To assess the behaviour of the BIST system, the energy demands of buildings with BIST and without have been compared. The results obtained are shown in terms of percentage of monthly energy saved or gained. Different passive strategies such as external shading in the windows of the south façade and ventilation at night (only when cooling is needed and the temperature of the exterior is lower than the assigned operative temperature) have been applied. The type56 and meteorological data from Energy Plus weather file have been used. The DHW demand has been determined assuming a water consumption of 30 litres per person at 60 ºC.

In order to compare the influence of the integration of BIST systems into buildings of new construction and in buildings already existing, it would be necessary to analyse the method by which the BIST would be installed in the new façade. This document does not deal with this procedure. In the present document the influence on the thermal envelope has been studied by adding a new material on the outside. The boundary temperature of the external wall has been considered as the temperature of the absorber. The covered area by the BIST systems has been considered to be 50% of the total area of the south façade.

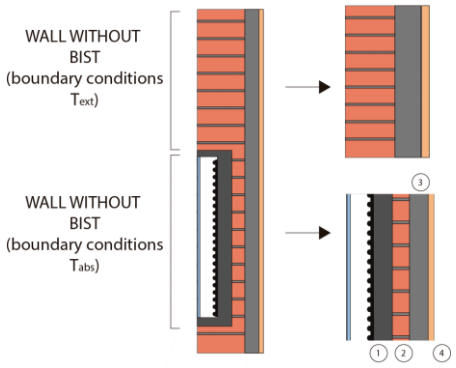

	Material	Density [kg/m^3]	Conductivity [W/m·K]	Heat capacity [J/kg·K]	Thickness [cm]
1	Insolation SC	*Variable depending of the prototype			
2	Solid brick	1920	0.72	835	7.5
3	Wool (insulation)	23	0.038	1800	Parametric
4	Plasterboard	800	0.17	----	1.5

Figure 3.5 Composition of the walls with BIST collector

The absorber temperature has been calculated at each time step (i) of the dynamic simulation with the approach methods suggested by Maurer et al. [6]. T_{abs} can be approximated by the average fluid temperature $T_{favg.}$ plus the thermal resistance between the average fluid temperature and the average absorber temperature R_{fa} multiplied by the useful collector gain $q_{use.}$

$$T_{abs,op,BIST}(i) = R_{fa}(i-1) \cdot q_{use,BIST}(i) + T_{fav}(i) \quad \text{eq. 9}$$

Where

$$T_{fav}(i) = T_{in}(i) + (T_{in}(i) + T_{out}(i))/2 \quad \text{eq. 10}$$

$$R_{fa}(i-1) = \frac{T_{abs,op,BIST}(i-1) - T_{fav}(i-1)}{q_{use,BIST}(i-1)} \quad \text{eq. 11}$$

When there is no fluid flow, the stagnation temperature has been calculated using the coefficients of the BIST collector described in the section 3.1.

$$T_{abs,stag,BIST}(i) = \Delta T_{stag,BIST} + T_a \frac{= -a_{1,BIST} + \sqrt{a_{1,BIST}^2 + 4a_{2,BIST} G \cdot \eta_{0,BIST}}}{2a_{2,BIST}} \quad \text{eq. 12}$$

3.4. TRNSYS model

TRNSYS 16 has been utilized for the simulation. This software includes a library of various built-in components often validated by experimental data. The system model shown in Figure3.6 shows the principal components that have been used. The solar thermal collector has been modelled by type 1b and the principal parameters have been calculated with the equations showed in section 3.2. To model the storage tank, type 534 from TESS libraries has been used. This tank could be used for domestic hot water, space-heating and it can also control the flow diverter (type 11) in which the tank heat exchanger (top or bottom) get across. To consider the influence of the collector temperature (absorber) on the thermal behavior of the building (Type56), to conduct the approximation of temperature of the absorber, showed in the section 3.3 has been used calculators and input value recall (type 93), this temperature has been linked to input created for (type56) through the interface TRNBUILD. The simulation also requires additional components such us; weather climate data (type 15-6), pumps, controllers (type 2), auxiliary heaters (type 6), data readers (type9) to conduct a global analysis of system.

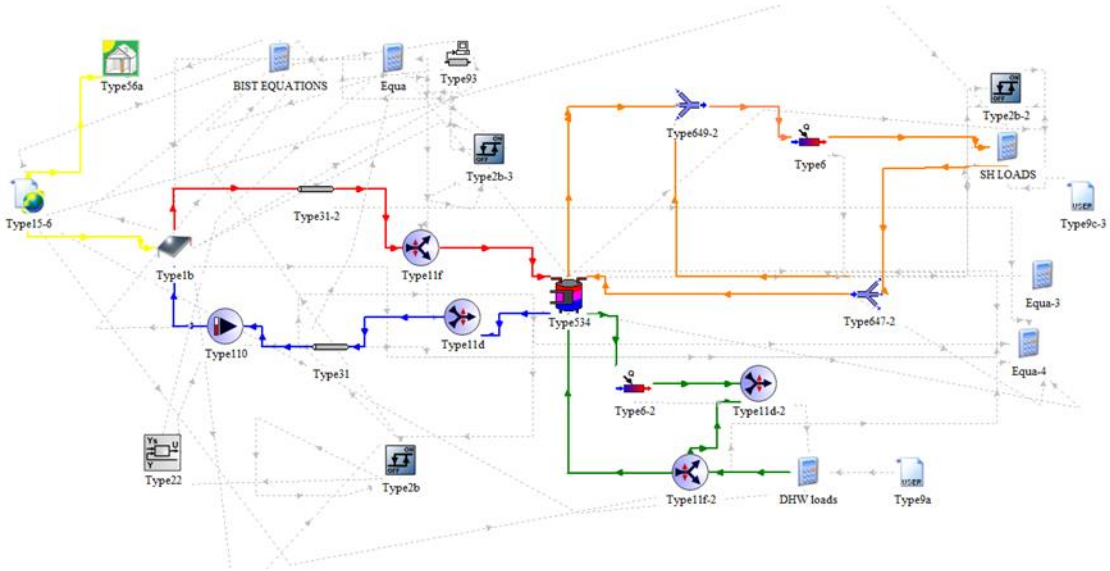

Figure 3.6 Trnsys Model

4. Results

4.1. Thermal demand of the building

In table 4.1, the summary of the simulated energy needs for heating, cooling and DHW for the single house are shown. These values are the reference to evaluate the energy impact of BIST systems.

Country	City	End-use	Jan	Feb	Mar	Apr	May	Jun	Jul	Aug	Sep	Oct	Nov	Dec	Annual	Total EN
ES	Madrid	Heating	30.8	23.7	16.1	12.4	2.3	0	0	0	1.0	8.0	20.0	31.4	145.7	176.5 kWh/m²
		Cooling	0.0	0.0	0.0	0.0	0.0	1.2	7.4	6.1	0.6	0.0	0.0	0.0	15.3	
		DHW	1.7	1.3	1.5	1.4	1.4	1.2	1.0	1.1	1.0	1.1	1.3	1.5	15.5	
IT	Rome	Heating	25.4	19.1	14.6	6.8	1.4	0.0	0.0	0.0	0.0	4.5	12.4	23.7	107.9	140.7 kWh/m²
		Cooling	0.0	0.0	0.0	0.0	0.1	1.9	6.9	7.1	1.3	0.7	0.0	0.0	18	
		DHW	1.5	1.2	1.4	1.1	1.1	1.2	1.3	1.2	1.2	1.1	1.1	1.4	14.8	
RO	Bucharest	Heating	44.3	31.9	22.7	6.9	1.8	0.0	0.0	0	2.3	12.8	29.6	40.9	193.2	226.6 kWh/m²
		Cooling	0.0	0.0	0.0	0.0	1.1	3.5	6.7	5.1	0.1	0.1	0.0	0.0	16.6	
		DHW	1.9	1.5	1.6	1.5	1.5	1.3	1.1	1.1	1.1	1.2	1.4	1.6	16.8	
AT	Vienna	Heating	28.5	23.6	13.4	5.5	0.8	0.0	0.0	0.0	0.8	7.0	19.3	29.1	128	156.7 kWh/m²
		Cooling	0.0	0.0	0.0	0.9	0.8	1.7	4.2	4.0	0.1	0.0	0.0	0.0	11.7	
		DHW	1.9	1.5	1.6	1.5	1.5	1.3	1.1	1.2	1.1	1.2	1.4	1.7	17	
FR	Paris	Heating	42.4	35.1	27.1	14.6	4.6	1.1	0	0	3.7	15.9	31.8	41.3	217.6	240.7 kWh/m²
		Cooling	0.0	0.0	0.0	0.0	0.1	0.8	3.3	2.3	0.0	0.0	0.0	0.0	6.5	
		DHW	1.8	1.4	1.6	1.5	1.5	1.3	1.1	1.2	1.1	1.2	1.3	1.6	16.6	
DE	Berlin	Heating	28.8	26.7	17.9	8.0	2.3	0	0.0	0	1.5	10.0	22.4	28.4	146	170.1 kWh/m²
		Cooling	0.0	0.0	0.0	0.0	0.3	2.4	2.9	1.4	0.0	0.0	0.0	0.0	7	
		DHW	1.8	1.4	1.6	1.5	1.5	1.4	1.2	1.2	1.2	1.3	1.4	1.6	17.1	
FI	Helsinki	Heating	26.7	23.0	17.5	7.3	1.0	0.0	0.0	0	3.7	12.3	23.2	27.0	141.7	160.4 kWh/m²
		Cooling	0.0	0.0	0.0	0.0	0.0	0.1	0.5	0.3	0.0	0.0	0.0	0.0	0.9	
		DHW	1.9	1.5	1.7	1.6	1.6	1.4	1.2	1.3	1.2	1.3	1.4	1.7	17.8	

Table 4.1 Heating/cooling and domestic hot water demand of the reference building.

The demand for heating and cooling varies depending on the city analyzed due to climatic conditions and characteristics of the different enclosures. The months with the warmest temperatures are from June to September, being July and August, when the thermometer reaches the highest temperatures. The winter months are mild. Rome with a mild Mediterranean climate. Madrid can be considered a transitional climate between a semi-arid climate and a Mediterranean climate with colder winters and hot summers. Bucharest has a mild continental climate, the weather is warm from June to September but in the winter months they are cold. Vienna presents a climate of transition, the center europe climate influenced by the Atlantic climate, hot summers and moderately cold winters. The climate of Paris is semicontinental oceanic, winters are cold and summers are moderately hot. The climate of Berlin is humid continentalwith cold winters and mild summer. Helsinki has an extremely cold winter climate and mild summers.

The energy demand for air conditioning not only depends on the climate, since the type of insulation of each country plays a very important role. Due to this, in a cold climate like Helsinki, the demand for heating is similar to Berlin or Spain. This fact would seem strange but it is due to a better insulation of the enclosures.

Regarding the DHW demand, the differences are shorter. There is more demand in the colder countries due to a lower water temperature network. This variability of climates will allow us to analyze the main types of climate that we find in Europe.

4.2. BIST

In the same way, the thermal demand with the BIST system has been evaluated and also the fraction of the domestic hot water and space-heating demand (SH) that solar thermal collectors cover.

Country	City	End-use	Jan	Feb	Mar	Apr	May	Jun	Jul	Aug	Sep	Oct	Nov	Dec	Annual	Total
ES	Madrid	Heating	28.8	28.8	21.8	14.4	10.9	1.8	0	0.0	0	0.7	6.8	18.3	132.3	164.6 kWh/m²
		Cooling	0.0	0.0	0.0	0.0	0.0	0.0	1.4	7.8	6.5	0.9	0.0	0.0	16.6	
		DHW	1.6	1.6	1.3	1.5	1.2	1.2	1.2	1.3	1.3	1.2	1.1	1.2	15.7	
IT	Rome	Heating	22.5	16.6	12.3	5.4	1.1	0.0	0.0	0.0	0.0	3.7	10.5	20.9	93	127 kWh/m²
		Cooling	0.0	0.0	0.0	0.0	0.2	2.1	7.0	7.4	1.6	0.9	0.0	0.0	19.2	
		DHW	1.5	1.2	1.4	1.1	1.1	1.2	1.3	1.2	1.2	1.1	1.1	1.4	14.8	
RO	Bucharest	Heating	41.7	29.6	20.6	5.7	1.4	0.0	0.0	0	1.8	11.5	27.7	38.5	178.5	214.4 kWh/m²
		Cooling	0.0	0.0	0.0	0.1	1.4	4.0	7.4	5.9	0.2	0.2	0.0	0.0	19.2	
		DHW	1.7	1.4	1.6	1.3	1.3	1.3	1.5	1.4	1.3	1.2	1.2	1.5	16.7	
AT	Vienna	Heating	26.8	21.9	11.7	4.6	0.5	0.0	0.0	0.0	0.6	6.1	17.9	27.5	117.6	148.9 kWh/m²
		Cooling	0.0	0.0	0.0	1.2	1.1	2.1	5.0	4.8	0.1	0.0	0.0	0.0	14.3	
		DHW	1.7	1.4	1.6	1.3	1.3	1.4	1.5	1.4	1.3	1.2	1.3	1.6	17	
FR	Paris	Heating	38.3	31.4	23.9	12.4	3.6	0	0	0	2.8	13.6	28.4	37.2	191.6	214.6 kWh/m²
		Cooling	0.0	0.0	0.0	0.0	0.1	0.8	3.3	2.4	0.0	0.0	0.0	0.0	6.6	
		DHW	1.6	1.3	1.5	1.3	1.3	1.3	1.5	1.4	1.3	1.2	1.2	1.5	16.4	
DE	Berlin	Heating	27.2	25.0	16.3	6.8	1.9	0	0.0	0.0	1.1	8.8	20.9	26.9	134.9	160.6 kWh/m²
		Cooling	0.0	0.0	0.0	0.1	0.4	2.7	3.4	1.8	0.1	0.0	0.0	0.0	8.5	
		DHW	1.7	1.4	1.6	1.3	1.3	1.4	1.6	1.5	1.4	1.2	1.3	1.5	17.2	
FI	Helsinki	Heating	26.0	22.2	16.6	6.5	0.9	0.0	0.0	0.0	3.2	11.7	22.6	26.4	136.1	156.2 kWh/m²
		Cooling	0.0	0.0	0.0	0.0	0.0	0.2	0.8	0.4	0.0	0.0	0.0	0.0	1.4	
		DHW	1.8	1.5	1.7	1.5	1.4	1.5	1.7	1.6	1.5	1.4	1.4	1.7	18.7	

Table 4.2 Heating/cooling and domestic hot water demand with the BIST system.

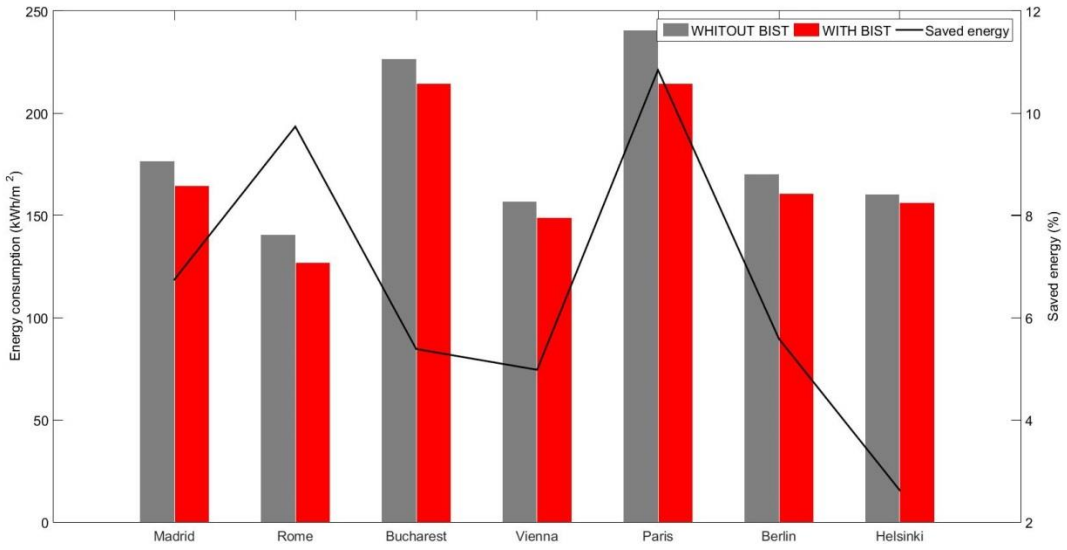

Figure 4.1 Total energy consumption with BIST and percentage of reduction thermal demand

The installation of BIST collectors reduces the thermal demand due to the increased insulation layer and the collector temperature, which is higher than the exterior temeprature. This high temperature in summer is not benefitial since it increases de refrigeration demand.

However, in the annual balance, the BIST system reduces the energy demand, outweighting all the extra

losses in summer as it can be seen in Fig4.1.

Therefore,

The DHW energy demand has to be satisfied prior to the SH demand. To evaluate the percentage of DHW demand that is covered by the BIST, the solar fraction is defined as:

$$SF_{DHW} = 100\left(1 - \frac{Consumption_{auxiliary,DHW}}{Demand\ DHW}\right)$$

The solar production aims at partially covering the SH demand, taking into consideration that the collector total area is quite low, approximately 25.5 m^2. The heating system considered is a radiant floor which impulsion temperature is assumed to be 42 °C and the return one to be 34 °C. In an analogous manner than in the DHW, the solar fraction covering the SH demand is expressed as:

$$SF_{SH} = 100\left(1 - \frac{Consumption_{auxiliary,DHW}}{Demand\ DHW}\right)$$

Country	City	End-use	Jan	Feb	Mar	Apr	May	Jun	Jul	Aug	Sep	Oct	Nov	Dec
ES	**Madrid**	SF_{DHW} [%]	79.3	93.7	98.9	94.4	98.6	100.0	100.0	100.0	97.5	98.1	95.8	76.1
		SF_{SH} [%]	10.0	11.2	14.0	9.6	17.2	-	-	-	-	18.9	13.4	6.61
IT	**Rome**	SF_{DHW} [%]	73.7	93.2	95.9	96.0	94.8	99.7	99.9	100.0	100.	97.7	91.2	84.3
		SF_{SH} [%]	7.4	10.5	10.3	9.7	16.6	-	-	-	-	7.7	10.4	7.0
RO	**Buchare**	SF_{DHW} [%]	73.9	91.1	92.0	98.7	99.9	100.0	100.0	100.0	100.	92.2	67.9	69.7
		SF_{SH} [%]	2.9	7.7	8.1	9.4	11.3	-	-	-	19.8	7.4	4.1	3.0
AT	**Vienna**	SF_{DHW} [%]	57.5	79.6	91.0	97.4	98.8	100.0	100.0	99.7	99.9	79.7	76.1	46.6
		SF_{SH} [%]	1.5	5.6	5.3	6.2	14.1	-	-	-	18.8	7.0	3.0	0.9
FR	**Paris**	SF_{DHW} [%]	52.1	65.7	81.8	96.1	99.9	99.6	99.3	100.0	99.4	92.9	69.8	51.3
		SF_{SH} [%]	2.2	4.9	4.8	7.2	9.4	-	-	-	14.6	6.7	3.0	1.1
DE	**Berlin**	SF_{DHW} [%]	46.5	58.5	81.3	98.5	99.3	100.0	99.9	100.0	98.8	84.7	69.2	35.1
		SF_{SH} [%]	0.8	4.4	3.6	8.3	7.8	-	-	-	22.5	5.5	4.0	0.8
FI	**Helsinki**	SF_{DHW} [%]	38.8	68.6	76.8	95.2	99.9	100.0	100.0	100.0	95.8	74.6	28.7	9.7
		SF_{SH} [%]	0.1	3.4	3.9	7.7	40.7	-	-	-	11.3	3.4	0.2	0.0

Table 4.3 Percentage of the solar fraction of the domestic hot water and space heating demand.

In climates with Mediterranean influence, total coverage of the domestic hot water is obtained whereas the contribution to the heating system is lower. There is heating demand mainly from November to February, and a coverage of 10% is reached. Bucharest and Vienna can be considered as transitional climates between Madrid or Rome and cooler climates like Paris or Berlin. Domestic hot water coverage is around 100% all year, except December and January. The contribution to the heating system is around 7%. Paris and Berlin, climates with less radiation, the coverage of domestic hot water is reduced, obtaining the 100% coverage only in the hotter months and values around 50% in the colder ones. The space heating coverage is around 5%. In Helsinki, during winter the contribution of the solar thermal system is low due to the low solar radiation whereas in summer, the coverage of domestic hot water is 100%.

5. Conclusions

A building-integrated solar-thermal collector has been simulated. The BIST system has been placed in the south façade employing 50% of the façade area. The BIST collector has been analysed by the contribution to domestic hot water and space heating and the influence in the thermal demand of building where it's installed has also been analysed.

Two weather data sources have been analysed and compared, IWEC and METEONORM .It has been observed that the influence of the file chosen in some cases can vary the results. The simulations have been carried with IWEC data in 7 capital cities; Spain, Italy, Romania, Austria, France, Germany and Finland. This has allowed to evaluate the system in different climatic conditions.

The simulation has been carried out with TRNSYS 16. The BIST parameters have been calculated with the approximation suggested by Maurer et al. [7]. In addition, the BIST system has been coupled with DHW (Domestic Hot Water) and SH (Space Heating) circuits. To analyse its contribution to the house energy demand, the model was linked with TRNBUILD. The characteristics of the building envelope have been determined from the corresponding U-values obtained from the ENTRANZE project.

The annual reduction of thermal demand respect the building without BIST system is around 6.60% in Spain, 9.92% in Italy, 5.38% in Romania, 5.04% in Austria, 10.30% in France, 5.68% in Germany and 2.62% in Finland. In the case of the domestic hot water energy demand, which has been considered a priority, the average solar fractions found are around the 94.30% in Spain, 93.80% in Italy, 90.45% in Romania, 85.52% in Austria, 84.00% in France, 81.00% in Germany and 74.00% in Finland. On the other hand, the proposed system covers a part of the space heating demand where the solar fraction is in the period from October to March 11.90% in Spain, 9.00% in Italy, 6.00% in Romania 4.21% in Austria, 4.20% in France, 3.90% in Germany and 2.60% in Finland.

Installing collectors as part of the southern façade can be beneficial in winter but counterproductive in summer, especially in climates with higher latitudes in which the installation of the BIST systems, reach higher temperature due to a greater irradiance on the vertical collectors.

After this work it is concluded the importance of continuing to work on the development of models that predict the behaviour of the BIST system and its validation with real systems. Also is necessary study the best way to include these systems in existing buildings or new buildings.

6. References

[1] EU, "Directive 2010/31/EU of the European Parliament and of the Council of 19 May 2010 on the energy performance of buildings (recast)," *Off. J. Eur. Union*, pp. 13–35, 2010.

[2] N. Carlisle, O. Van Geet, and S. Pless, "Definition of a ' Zero Net Energy ' Community," *Natl. Renew. Energy Lab.*, no. November, pp. 1–14, 2009.

[3] NREL, "No Title," *https://www.nrel.gov/workingwithus/re-solar.html*. .

[4] "Annual_Report_Fraunhofer_ISE_2015-2016," 2015.

[5] G. Leone and M. Beccali, “Use of finite element models for estimating thermal performance of fa??ade-integrated solar thermal collectors,” *Appl. Energy*, vol. 171, pp. 392–404, 2016.

[6] C. Maurer, C. Cappel, and T. E. Kuhn, “Simple models for building-integrated solar thermal systems,” *Energy Build.*, vol. 103, pp. 118–123, 2015.

[7] I. Visa, A. Duta, M. Comsit, M. Moldovan, D. Ciobanu, R. Saulescu, and B. Burduhos, “Design and experimental optimisation of a novel flat plate solar thermal collector with trapezoidal shape for facades integration,” *Appl. Therm. Eng.*, vol. 90, pp. 432–443, 2015.

[8] I. Visa, M. Moldovan, M. Comsit, M. Neagoe, and A. Duta, “Facades Integrated Solar-thermal Collectors – Challenges and Solutions,” *Energy Procedia*, vol. 112, no. October 2016, pp. 176–185, 2017.

[9] P. I. Cooper and R. V. Dunkle, “A non-linear flat-plate collector model,” *Sol. Energy*, vol. 26, no. 2, pp. 133–140, 1981.

[10] “ENTRANZE :: Data Tool.” [Online]. Available: http://www.entranze.eu/tools/interactive-data-tool. [Accessed: 22-May-2017].